ISSN 1054-660X, Laser Physics, 2006, Vol. 16, No. 5, pp. 741–746.

Fluorescence Diffuse Tomography of Small Animals with DsRed2 Fluorescent Protein

I. V. Turchin[a, *], V. I. Plehanov[a], A. G. Orlova[a], V. A. Kamenskiy[a], M. S. Kleshnin[a], M. V. Shirmanova[a], N. M. Shakhova[a], I. V. Balalaeva[a], and A. P. Savitskiy[b]

[a] *Institute of Applied Physics of RAS, Ulyanov st. 46, Nizhni Novgorod, 603950 Russia*

[b] *A. N. Bach Institute of Biochemistry of the RAS, Leninsky pr. 33-2, Moscow, 190071 Russia*

*e-mail: ilya@ufp.appl.sci-nnov.ru

Received December 26, 2005

Abstract—Fluorescent compounds are used as markers to diagnose oncological diseases, to study molecular processes typical for carcinogenesis, and to investigate metastasis formation and tumor regress under the influence of therapeutics. Different types of tomography, such as continuous wave (CW), frequency-domain (FD), and time-domain (TD) tomography, allow fluorescence imaging of tumors located deep in human or animal tissue. In this work, preliminary results of the frequency domain fluorescent diffuse tomography (FDT) method in application to DsRed2 protein as a fluorescent agent are presented. For the first step of our experiments, we utilized low-frequency amplitude modulation (1 kHz) of second harmonic of Nd:YAG (532 nm). The transilluminative configuration was used in the setup. The results of post mortem experiments with capsules containing DsRed2 inserted inside the esophagus of a 3-day-old hairless rat to simulate tumor are shown. An algorithm of processing fluorescent images based on calculating the zero of maximum curvature has been applied to detect fluorescent inclusion boundaries in the image. This work demonstrates the potential capability of the FDT method for imaging deep fluorescent tumors in human tissue or animal models of human cancer. Improvement of the setup can be accomplished by using high-frequency modulation (using a 110-MHz acoustooptical modulator).

PACS numbers: 42.30.Wb, 81.07.Ta

DOI: 10.1134/S1054660X06050021

1. INTRODUCTION

Strong light scattering and absorption limit the visualization of the internal structure of biological tissue. Only special tools for turbid media imaging, such as optical coherence tomography, optoacoustics, and optical diffusion tomography (ODT), enable noninvasive investigation of the internal structure of biological tissue [1]. ODT is based on information acquisition from diffused (multiply scattered) photons, which penetrate to a depth of up to several centimeters inside tissue. This technique allows the absorbing and scattering inhomogeneities inside tissue to be visualized; the reconstruction of the tissue structure is based on processing the detected light, which is diffusively transmitted through the scattering medium. Creation of new light sources and optical modulators have stimulated the development of a novel modification of ODT, the so-called frequency domain optical diffusion tomography, which employs illumination of the tissue by amplitude-modulated light [2, 3]. This method significantly increases the spatial resolution of the observed objects inside turbid medium due to registration and processing of the amplitude and phase of signal envelope, which both carry information about the tissue structure.

Various tissue structures and their alterations can be observed with higher contrast due to the fluorescence effect. In this case, illumination of the investigated object is performed at the wavelength from the region of absorption, and the useful signal is detected at the wavelength from the emission spectrum region, which are well separated. Exogenous fluorophores targeted specifically at tumor cells and fluorescent proteins (FPs) expressed endogenously are utilized as markers in medical and biological investigations.

Currently, one of the basic applications of fluorescent proteins is monitoring tumor growth, angiogenesis, metastasis formation, and the effects of new classes of drugs. A gene of FP is transduced to human cancer cells, and genetically modificated human cancer cell lines are injected into immunodeficient nude mice. Such human xenograft tumor models allow the growth characteristics and metastasis of donor human tumors to be imitated in a whole animal system and provide many new possibilities for research, including real-time studies of drug-response evaluations [4–7]. Synthesis and fluorescence ability of FPs persist for the whole life of cancer cells and remain after cell division. FPs allow the permanent visual monitoring of cancer tumor growth inside intact animals to be performed without the necessity of anesthesia, substrate injection, or contrasting agents. The fundamental advantage of FPs is the possibility of their usage when investigating living,

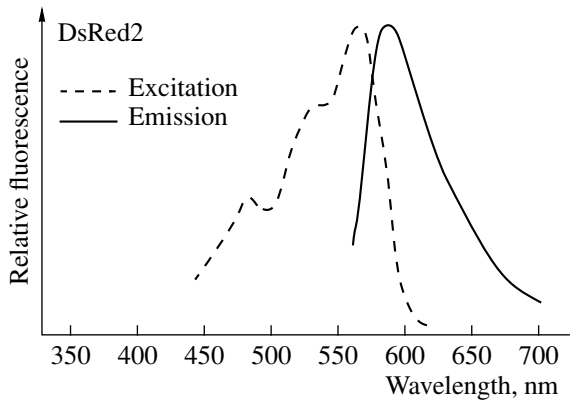

Fig. 1. Excitation (dotted line) and emission (solid line) spectra of DsRed2 fluorescent protein [20].

developing cells. The method has been approved on various models, such as models of pancreas cancer, Lewis lung carcinoma and other lung tumors, breast cancer, prostate cancer, melanoma, brain cancer, etc. [2–5]. The green fluorescent protein (GFP) was one of the first fluorescent proteins to be used for in vivo imaging. A drawback of GFP is its short emission wavelength, which overlaps with the autofluorescence of many tissues. With GFP, imaging is limited to a few millimeters [8]. Recently, a new red fluorescent protein (DsRed2) has been isolated. The fluorescence spectrum of this protein is shifted into the relatively long-wave part of spectrum (580 nm), which is promising for object visualization at depths up to 1–2 cm with millimeter resolution [9].

Such an experiment layout requires development of methods for intravital observation of alteration of FP-labeling tumors located deep in tissue. Whole-body fluorescence images are usually acquired using a CCD camera focused on the skin surface of the animal [10, 11]. Such detection sensitivity, however, is confined to tissue that lies close to the skin surface. The fluorescence from deeper lying tissue is rapidly attenuated through absorption and scattering of the fluorescing light.

Different types of fluorescent tomography—time domain (TD), frequency domain (FD), or fluorescent diffuse photon density waves, and continuous wave (CW)—account for the diffusive propagation of photons in tissue [11–16]. The use of theoretical models of photon propagation in tissues and subsequent mathematical inversion makes possible the determination of real boundaries of tumors located deep in an animal with high resolution. These techniques have been utilized for investigation of the distribution of near-infrared fluorescent probes [13–16] and fluorescent proteins in visible light on model tumors in vivo [17]. In this work, the results of preliminary experiments with DsRed fluorescent protein in model media and in small animals utilizing FDT experimental setup with low-frequency modulation are shown [18]. We use the transilluminative configuration of scanning a rat. As excitation light, we used second-harmonic generation of a Nd:YAG laser at 532 nm, which is close to the maximum of absorbance of DsRed2. The emission spectral range of DsRed2 is 540–650 nm. An algorithm based on the calculation of the zero of maximum-curvature lines of fluorescent images was used to detect the boundaries of fluorescent inclusions. The results of FDT experiment using high-frequency modulation (110 MHz) performed using an acoustooptical modulator and image reconstruction algorithm based on the method of the mean paths of photons [19] are now under analysis.

2. MATERIALS AND METHODS

Preliminary experiments with FDT were performed using DsRed2 fluorescent protein. The emission and excitation spectra of DsRed2 are shown in Fig. 1. In the experimental setup (Fig. 2), low-frequency modulated light (f_0 = 1 kHz) from a Nd:YAG laser with second-harmonic generation at a wavelength of 532 nm, which is close to the absorption maximum of FP, was used. The power on the object under investigation was 12 mW, the beam diameter was 2 mm, aperture of the detector was 1.5 mm, and the numerical aperture of the detector was 0.22. As a detector, we used a Hamamatsu H7422-20 high-sensitivity cooled photomultiplier tube (PMT). A combination of interferometric and absorption filters was used to separate emission (535–585 nm) and excitation (605–685 nm) spectra. The suppression of excitation spectra at the detector's input of the PMT module was equivalent to 6 optical densities.

Synchronous scanning of the object in the transilluminative configuration was provided by a single pair of source and detector set in motion by stepping motors. The device was controlled by computer. A black box, which covers the scanning system, was used to eliminate the ambient light that results in additional noise on the FDT image. To perform mode-locked detection for low-frequency modulation, no different frequency was needed (Δf = 0): the fluorescent signal and reference signal can be digitized simultaneously by ADC without mixing. For high-frequency modulation, an additional oscillator with shifted frequency ($f_0 + \Delta f$) is needed to perform mode-locked detection (Fig. 3). The shifted frequency can be also obtained using a frequency synthesizer. The FDT experimental setup is shown in Fig. 4.

3. RESULTS

A series of model and *post mortem* experiments has been conducted using the FDT setup with low-frequency modulation.

Model Experiment

Figure 5 shows the scheme of the scanning model media—a quartz box with sizes of 50 × 27 × 19 mm

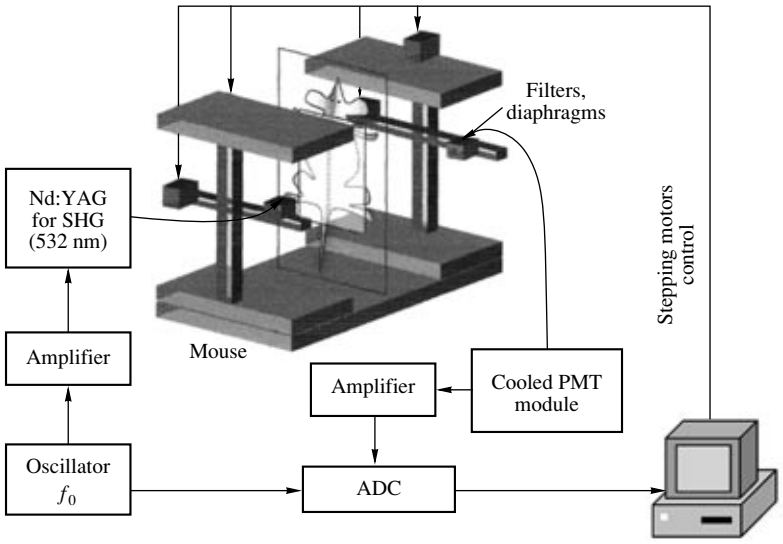

Fig. 2. Scheme of the low-frequency FDT experimental setup.

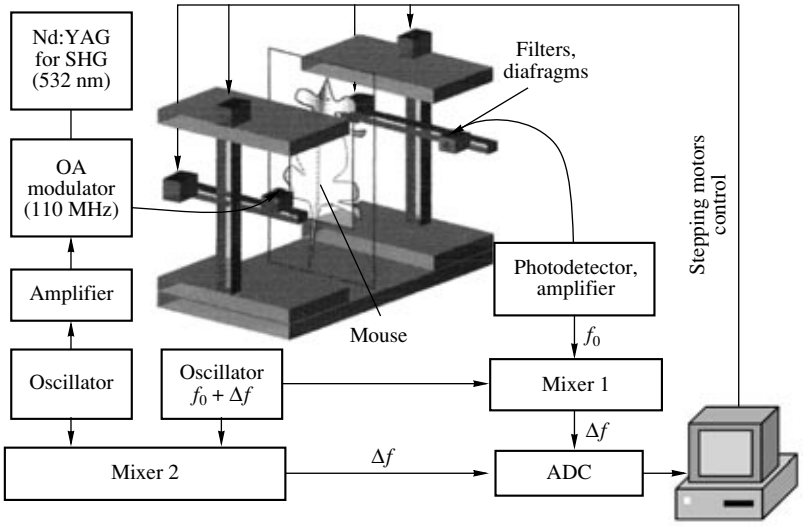

Fig. 3. Scheme of the high-frequency FDT experimental setup.

(W × H × D) containing a water solution of intralipid and India ink. The absorption coefficient of this medium was 0.5 cm^{-1} and the reduced scattering coefficient was 15 cm^{-1}, which are close to the averaged scattering parameters of biotissue [17]. A glass capsule with an internal diameter of 2.5 mm containing DsRed2 at a concentration of 10^{-5} M/1 was placed in the box's center. Polystyrene beads of 1 μm (Bangs Laboratory) were added in the DsRed solution to provide the same scattering parameters in the capsule as in the surrounding medium. It is clearly seen from Fig. 6 that the selectivity of the system is enough high to separate light at excitation and emission wavelengths.

Post Mortem Experiments

The results of *post mortem* experiments are shown in Fig. 7. The glass capsule containing DsRed2 was inserted inside the esophagus of a euthanized 3-day-old hairless rat (18–20 g) to simulate a tumor. The concentration of DsRed2 solution was 10^{-6} M/1 in citrate-phosphate buffer (pH 8.5). The internal diameter of the capsule with DsRed2 was 2.5 mm. During the experiment, an animal was placed vertically in the container, which consists of a supporting plate and the covering plate and which was slightly pressed to fix the animal (Fig. 7a). The distance between plates was 1 cm. A series of additional in vivo experiments with mice and rats (without any capsules) were conducted, and it was

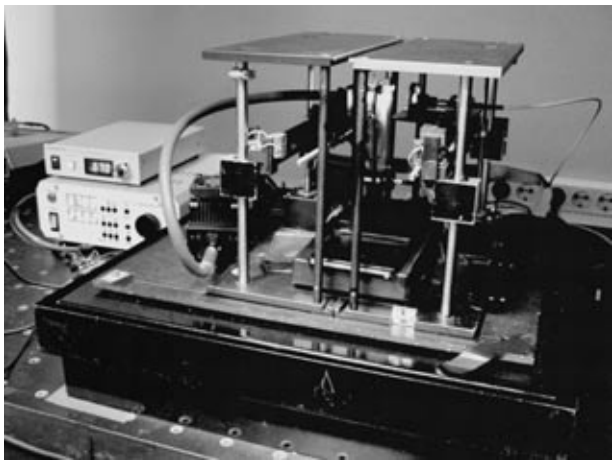

Fig. 4. FDT experimental setup created at the Institute of Applied Physics, Russia.

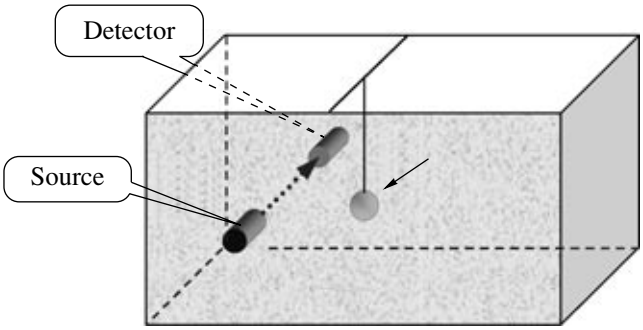

Fig. 5. Scheme of the model experiment with FDT: a glass capsule (marked with an arrow) containing DsRed suspension was placed in water solution of intralipid and India ink.

shown that such a configuration does not traumatize the animal. It is clearly seen from Fig. 7 that the capsules have a high contrast in the images. It should be noted that the surrounding area of the mouse looks bright due to the high power of light emission that is directly transmitted to the detector in this part of the plot. It was found that the high fluorescence signal is also due to the large difference in the scattering parameters of the fluorescing capsule and the surrounding tissues.

In order to approach the conditions of a real experiment with fluorescing tumors, we conducted an experiment with a glass capsule containing DsRed2 and a solution of 1-μm polystyrene beads. The solution in the capsule has scattering characteristics (reduced scattering and absorption coefficients) close to those in biotissue. The concentration of DsRed2 in the capsule was 5×10^{-6} M/1. A comparison of FDT images obtained for scattering and nonscattering capsules is shown in Figs. 8a and 8c, respectively. Due to high scattering, the signal from the fluorescing capsule is 2.3 times higher than in the nonscattering capsule. Taking into account that the concentration in the second case was 5 times lower, the scattering decreases the fluoresce signal by approximately 10 times.

Detection of Fluorescing Inclusion Boundaries

In order to perform automated detection of fluorescent inclusion boundaries, one can use the maximum curvature k_{max} [21]. The function $k_{max}(x, y)$ can be calculated using a second-order local approximation of the fluorescence image surface $z(x, y)$. Zero points of the maximum curvature $k_{max}(x, y) = 0$ describe the boundaries of fluorescence inclusions on the FDT image. An example of the function $k_{max}(x, y)$ corresponding to $z(x, y)$ (at fixed coordinate y, shown in Fig. 8a as a dashed line) is shown in Fig. 9. The peak of the fluorescence signal (dotted line in Fig. 9) corresponds to the center point of capsule in Fig. 8a. As shown in Figs. 8b and 8d, the detected boundaries (black lines) of the fluorescent inclusion have the same size in spite of the significant difference in the fluorescence signal.

4. CONCLUSIONS AND FUTURE DIRECTIONS

Preliminary experiments with DsRed2 fluorescent protein using an experimental setup with low-frequency modulated light have shown the potential capability of the

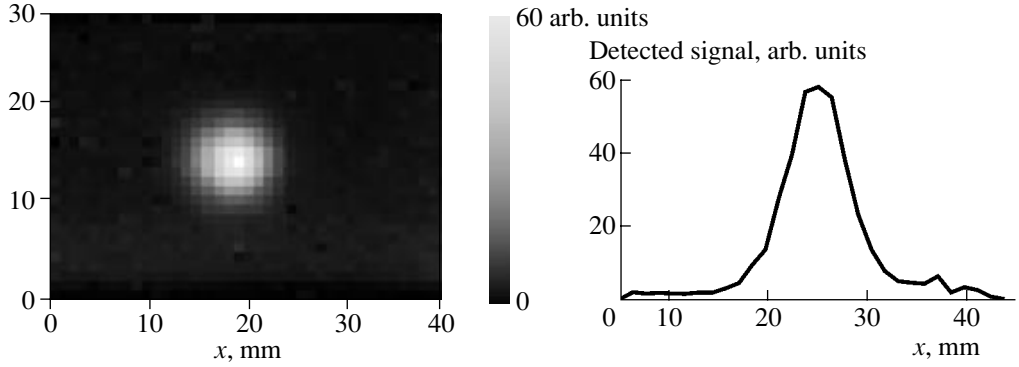

Fig. 6. FDT image of model media shown on Fig. 5.

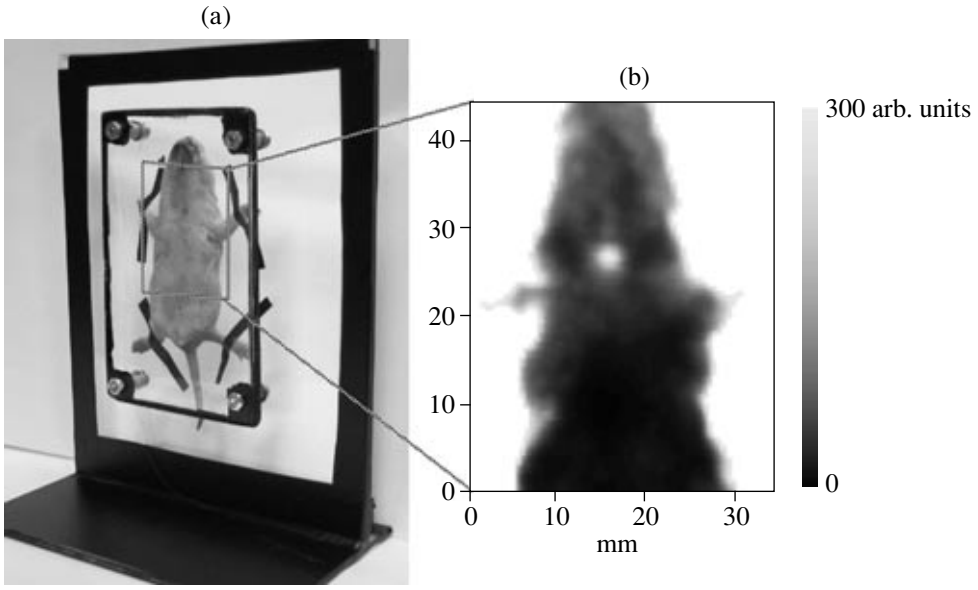

Fig. 7. Plot (a) shows the scheme of FDT experiments with small animals: an animal is placed vertically in the container, which consists of a supporting plate and a covering plate which are slightly pressed to fix the animal. Plot (b) shows the FDT image of the glass capsule with an internal diameter of 2.5 mm containing fluorescent protein DsRed2 suspension after insertion inside the esophagus of a rat. The concentration of DsRed2 solution was 10^{-6} M/1.

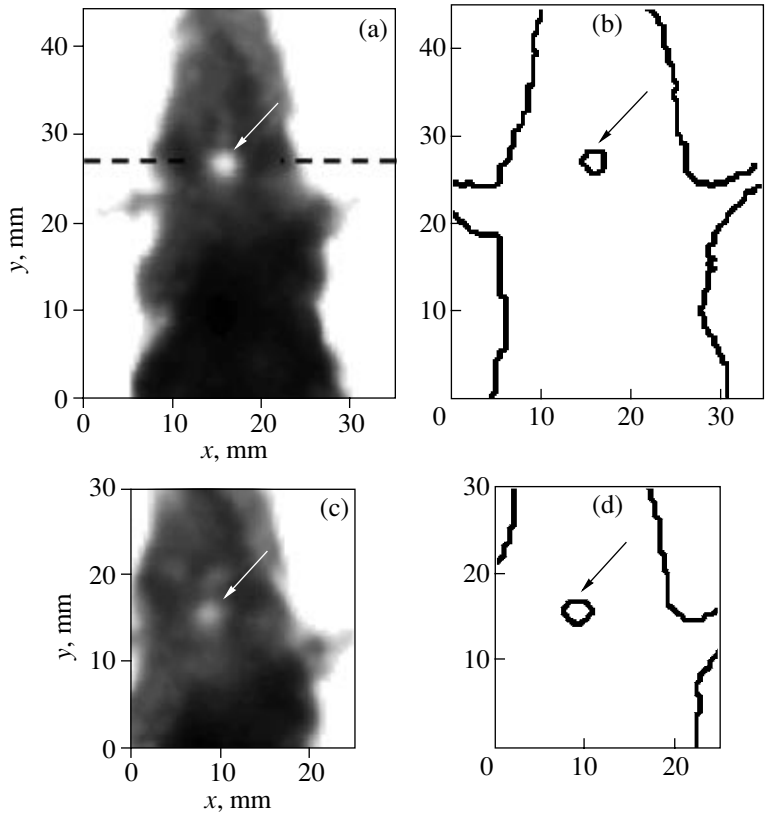

Fig. 8. Plots (a) and (c) show the FDT images of the glass capsule containing DsRed2 suspension with an internal diameter of 2.5 mm after insertion inside the esophagus of a rat. The concentration of DsRed2 solution was (a) 10^{-6} M/1 and (c) 5×10^{-6} M/1. In the experiment (c) 1-μm polystyrene beads have been added in the capsule in order to equalize the scattering properties in the capsule and the surrounding media. Plots (b) and (d) show the results of processing (a) and (c), respectively. The black lines in images (b) and (d) correspond to the detected boundaries of fluorescent inclusions (capsules). These boundaries were obtained using zero-maximum-curvature lines of image surfaces (a) and (b). Arrows show the location of fluorescing capsules.

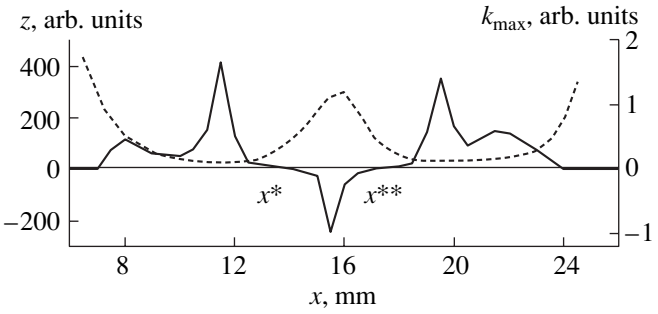

Fig. 9. Maximum curvature k_{max} (solid line) as a function of coordinate x calculated for the image surface $z(x, y)$ shown in Fig. 8a (this section corresponds to the dashed line in Fig. 8a). The dashed line shows z as a function of x. The zero points x^* and x^{**} of k_{max} show the boundaries of the capsule in Fig. 8a.

FDT method for imaging deep fluorescent tumors in vivo at depths of 0.5–1.5 cm. Using the zeros of maximum curvature, it is possible to detect the "true" tumor boundaries and to quantitatively estimate the tumor growth in vivo. As shown in Figs. 8b and 8d, this algorithm is not sensitive to the value of the fluorescence signal.

The described experimental approach does not require additional study to determine the form and the size of the fluorescent object and the fluorophore concentration. At the same time, during the experiment, the light penetrates heterogeneous animal tissues, so that the obtained results are more reliable in comparison with the typical case using homogeneous phantoms. The described model system provides conditions identical to realistic ones and makes it possible to carry out in vivo observation of molecular processes typical for the propagation and regress of a deep FP-labeled tumor on animal models of human cancer. The proposed method of fixing an animal is convenient for scanning in the transilluminative configuration and makes it easy to solve the inverse tomographic task, since the boundaries are plane. A series of additional in vivo experiments with mice and rats (without any capsules) were conducted, and it was shown that this configuration does not traumatize the animal.

However, the concentration of FP in model media was too high (10^{-6}–5×10^{-6} M/l) in comparison with the typical concentration for a fluorescent tumor (10^{-7} M/l). The sensitivity of the system is high enough to detect concentrations of 10^{-8}–10^{-7} M/l, but in this case the background signal which due to the fluorescence of surrounding tissues and the high power of transmitted light is comparable with the signal from the fluorescing capsule. In order to decrease the background signal, we will detect fluorescent and excitation light separately and subtract the excitation light. The selection of fluorescent and excitation light can be provided by a dichroic mirror placed in front of the detector. The use of high-frequency modulation (110 MHz) will provide an additional measuring parameter—the phase of the transmitted signal. In our opinion, this information will be useful to separate FP and surrounding tissue fluorescence. A 3D image reconstruction apparatus based on the method of the mean paths of photons [17] is now underway. Using the method of detection of boundaries of fluorescing inclusions, it will be possible to calculate the volume of the tumor after 3D reconstruction.

ACKNOWLEDGMENTS

This work was supported in part by the Russian Foundation for Basic Research (project nos. 04-02-16748, 05-02-20159, 05-08-50276, and 05-02-16748), Science and Innovations Federal Russian Agency (project nos. 02.435.11.3004 and 02.442.11.7142), the program of the Presidium of the Russian Academy of Sciences "Fundamental Sciences for Medicine," and the Molecular and Cellular Biology Program, Russian Academy of Sciences.

REFERENCES

1. A. M. Sergeev, L. S. Dolin, and D. H. Reitze, Opt. Photonics News, No. 7, 328 (2001).
2. S. Fantini, E. L. Heffer, H. Siebold, and O. Schutz, Opt. Photonics News, No. 11, 24 (2003).
3. Ch. Yu, Ch. Mu, X. Intes, and B. Chance, Opt. Express **9**, 212 (2001).
4. R. M. Hoffman, Lab. Animal **31**, 34 (2002).
5. M. Yang, E. Baranov, J.-W. Wang, et al., PNAS **99**, 3824 (2002).
6. M. Bouvet, J. Wang, S. R. Nardin, et al., Cancer Res. **62**, 1534 (2002).
7. M. H. Katz, S. Takimoto, D. Spivack, et al., J. Surg. Res. **113**, 151 (2003).
8. R. Weissleder and V. Ntziachristos, Nat. Med. **9**, 123 (2003).
9. M. V. Matz, A. F. Fradkov, Y. A. Labas, et al., Nat. Biotechnol. **17**, 969 (1999).
10. B. Rashidi, M. Yang, P. Jiang, et al., Clin. Exp. Metastasis **18**, 57 (2000).
11. M. H. Katz, S. Takimoto, D. Spivack, et al., Clin. Exp. Metastasis **21**, 7 (2004).
12. M. A. O'Leary, D. A. Boas, X. D. Li, et al., Opt. Lett. **21**, 123 (1996).
13. A. B. Milstein, J. J. Stott, D. A. Boas, et al., J. Opt. Soc. Am. A **21**, 1035 (2004).
14. V. Ntziachristos, J. Ripoll, L. V. Wang, and R. Wesslender, Nat. Biotechnol. **23**, 313 (2005).
15. V. Ntziachristos, E. A. Schellenberger, J. Ripoll, et al., PNAS **101**, 12294 (2004).
16. S. V. Patwardhan, S. R. Bloch, S. Achilefu, and J. P. Culver, Opt. Express **13**, 2564 (2005).
17. G. Zacharakis, J. Ripoll, R. Weissleder, and V. Ntziachristos, IEEE Trans. Med. Imaging **24**, 878 (2005).
18. I. V. Turchin, V. I. Plehanov, E. A. Sergeeva, et al., SPIE Proc. **5859-57**, 227 (2005).
19. V. Lyubimov, Opt. Spectrosc. **88**, 282 (2000).
20. G. Patterson, R. N. Day, and D. Piston, J. Cell Sci. **114**, 837 (2001).
21. D. C. Van Essen, H. A. Drury, S. Joshi, and M. Miller, Proc. Natl. Acad. Sci. USA **95**, 788 (1998).